

Document downloaded from:

<http://hdl.handle.net/10251/141959>

This paper must be cited as:

Fulladosa, E.; Austrich, A.; Muñoz, I.; Guerrero, L.; Benedito Fort, JJ.; Lorenzo, J.; Gou, P. (07-2). Texture characterization of dry-cured ham using multi energy X-ray analysis. Food Control. 89:46-53. <https://doi.org/10.1016/j.foodcont.2018.01.020>



The final publication is available at

<https://doi.org/10.1016/j.foodcont.2018.01.020>

Copyright Elsevier

Additional Information

Accepted Manuscript

Texture characterization of dry-cured ham using multi energy X-ray analysis

E. Fulladosa, A. Austrich, I. Muñoz, L. Guerrero, J. Benedito, J.M. Lorenzo, P. Gou

PII: S0956-7135(18)30026-4

DOI: [10.1016/j.foodcont.2018.01.020](https://doi.org/10.1016/j.foodcont.2018.01.020)

Reference: JFCO 5951

To appear in: *Food Control*



Please cite this article as: E. Fulladosa, A. Austrich, I. Muñoz, L. Guerrero, J. Benedito, J.M. Lorenzo, P. Gou, Texture characterization of dry-cured ham using multi energy X-ray analysis, *Food Control* (2018), doi: 10.1016/j.foodcont.2018.01.020

This is a PDF file of an unedited manuscript that has been accepted for publication. As a service to our customers we are providing this early version of the manuscript. The manuscript will undergo copyediting, typesetting, and review of the resulting proof before it is published in its final form. Please note that during the production process errors may be discovered which could affect the content, and all legal disclaimers that apply to the journal pertain.

Texture characterization of dry-cured ham using multi energy X-ray analysis

E. Fulladosa, A. Austrich, I. Muñoz, L. Guerrero, J. Benedito, J.M Lorenzo, Gou, P.

IRTA. XARTA. Food Technology programme. Finca Camps i Armet, s/n 17121 Monells, Girona, Catalonia.

CTC. Centro Tecnológico de la Carne, Rúa Galicia N°4, Parque Tecnológico de Galicia, San Cibrán das Viñas, 32900 Ourense, Spain.

UPV. Department of Food Technology, Universitat Politècnica de València, Camí de Vera s/n, E-46022 València, Spain.

Abstract – Multi energy X-ray sensors are able to differentiate and quantify X-rays of different energies. In contrast to conventional sensors, which simply record the overall energy of the X-rays whatever the energy of x-rays is, multi energy sensors provides a spectrum of the X-rays energies, which may be differently attenuated. In this study, the feasibility of this technology to detect changes in dry-cured ham slices after inducing proteolysis was evaluated. Effect of salt and water contents on the attenuation was also studied. In addition, the classification of commercial samples according to their proteolysis index was assessed. Results showed a decrease of attenuation for increasing proteolysis induction times ($p<0.01$) for all the regions of the spectrum (energy bands), but not with the same intensity, at any of the analysed acquisition conditions. Salt and water contents produced a significant ($p<0.01$) effect on the attenuation. Influence of salt content was higher than that of water content, and both affected the prediction of the proteolysis index. Classification score of commercial samples exhibited a limited discrimination capacity, showing the need for more sophisticated data analysis.

Key Words – non-destructive, quality evaluation, proteolysis, spectrometry

30 1. Introduction

31 Chemical and physical changes occur during the processing of dry-cured ham, impacting on the
32 final texture of this product and influencing consumer's acceptability (Morales, Guerrero,
33 Claret, Guàrdia, & Gou, 2008). These changes are strongly dependent on many factors such as
34 the raw material characteristics, genetics, the activity of proteolytic enzymes and the processing
35 conditions (Guerrero, et al., 2004; Schivazappa, et al., 2002; Skrlep, et al., 2011). The high
36 variability of these factors and the complex interrelation between them make it difficult to
37 control the correct development of the texture and gives rise to the development of texture
38 defects such as pastiness, which is highly related to the proteolysis intensity of the samples and
39 occurs in an important part of the dry-cured ham production (Tapiador Farello & García
40 Garrido, 2003). However, corrective treatments such as the application of mild thermal
41 treatments (Morales, Arnau, Serra, Guerrero, & Gou, 2008) or high pressure (Fulladosa, Sala,
42 Gou, Garriga, & Arnau, 2012) are able to reduce this defect. On this basis a rapid online method
43 capable of non-destructive detection of product with defective textures would enable application
44 of these corrective treatments prior to sale.

45 Several non-invasive technologies have the potential to determine textural features of dry-cured
46 meat products (Damez & Clerjon, 2013; Font-i-Furnols, Fulladosa, Prevolnik, & Candek
47 Potokar, 2015). In this regard, near infrared and microwave spectroscopy have been found able
48 to discriminate between dry-cured hams with pastiness and those with a normal texture (García-
49 Rey, García-Olmo, Pedro, Quiles-Zafra, & Castro, 2005; Ortiz, Sarabia, García-Rey, & Castro,
50 2006; Rubio-Celorio, Fulladosa, Claret, Guàrdia, & Garcia-Gil, 2013). Laser backscattering
51 imaging has also been found to be related to the proteolysis index of hams but, as in the case of
52 the previously mentioned technologies, many factors (especially water content) interfered with
53 its estimation (Fulladosa, Rubio-Celorio, Skytte, Muñoz, & Picouet, 2017). X-ray based
54 technologies, using single or dual absorptiometry, were proved to be useful for compositional
55 analysis of thick samples of dry-cured ham (De Prados, et al., 2015; Fulladosa, et al., 2015)
56 whereas salt content in sliced dry-cured ham could only be achieved using recently developed
57 multi energy sensors (Fulladosa, Gou, & Muñoz, 2016). In contrast to conventional sensors,
58 multi energy sensors are able to measure the energy of each transmitted photon and construct an
59 energy spectra over several energy channels. Information provided by these spectra might be
60 useful to analyze textural characteristics. However, no studies related to estimation of textural
61 characteristics using this type of X-ray sensors were found in literature.

62 The aim of this work was to evaluate the feasibility of multi energy X-ray spectrometry to detect
63 changes in sliced dry-cured ham after inducing proteolysis using a proteolytic enzyme. The
64 effect of proteolysis and salt and water contents on X-ray attenuation at different acquisition

65 conditions was analysed. The ability of the technology to characterize and classify commercial
66 samples according to their proteolysis index or defective texture level was also assessed.

67 2. Material and methods

68 2.1 Prototype device with multi energy X-ray detector

69 An X-ray system (MXV-MEAT 6025, Multiscan Technologies, Cocentaina, Spain) with a multi
70 energy detector was used to scan the samples (Figure 1). The prototype had an X-ray
71 spectrometric detector made of a semiconductor crystal (CDTe/CZT) with a pixel size of 0.8
72 mm. A belt conveyor transported the sample at a speed of 10 m/min. Simultaneously, X-rays
73 were emitted from below the samples using a tungsten X-ray tube which operates from 40 to
74 150 kV. The energy of the transmitted X-rays was measured at the upper part of the device
75 using the detector. The system acquired a spectroscopic image (1000 x 256 pixels) of the
76 sample with each pixel containing an X-ray energy spectra of 128 channels (recording energies
77 from 20 to 160 keV). The size of the acquired information was a 3D matrix consisting of 1000 x
78 256 pixels x 128 channels.

79 2.2 Extraction of ROI information: mean spectra and energy bands

80 In order to analyse the images, specific regions of interest (ROIs) from each sample, specifically
81 *Biceps femoris* muscle, were selected. The selected ROIs, in which each pixel contained an
82 energy spectrum, were analysed using a Matlab script written in house (MATLAB, Ver. 7.7.0,
83 The Mathworks Inc., Natick, MA, USA). The mean X-ray attenuation (S_a) for the energy
84 channel a of the selected ROI (Figure 2) was calculated after background correction and log-
85 transformation as described in equation 1.

$$86 \quad S_a = \frac{-\sum_{i=1}^p \ln\left(\frac{I_f^{a,i}}{I_o^{a,i}}\right)}{p} \quad (\text{Eq 1})$$

87 where I_f is the intensity of the transmitted radiation and I_o is the intensity of the incident
88 radiation at each pixel i of the ROI which contains p pixels. The calculation was done for each
89 energy channel a , which ranged from 1 to 128 and represented a given X-ray energy. According
90 to Eq 1, an increase of S_a value represents an increase of the X-ray attenuation for channel a .

91 There was a part of the spectra in which photons with energies higher than the maximum
92 applied keV were found. This was due to the pile up phenomenon (McCullough, Leng, Yu, &
93 Fletcher, 2015) and it was not included in the analysis.

94 Different Energy bands (EB) of the spectra, (x - y) being the given number of energy channels,
95 were selected (Figure 2). Energy band attenuation was calculated as the average attenuation of
96 the energy channels included in the energy band using equation 2;

$$EB_{x-y} = \frac{\sum_{a=x}^y S_a}{y-x+1} \quad (\text{Eq. 2})$$

98 x and y correspond to the first and last energy channel a of the energy band considered. In this
 99 study, energy bands investigated contained 20 channels resulting in the whole spectra being
 100 divided into 6 energy bands (Figure 2). Each energy band represents areas of the spectrum with
 101 different responses.

102 **2.3 Experimental protocols**

103 **2.3.1 Effect of induced proteolysis on multi energy X-ray spectra and energy bands**

104 The effect of sliced dry-cured ham exposure to a proteolytic enzyme on the X-ray spectra when
 105 using different acquisition conditions (140 kV and 1 mA, 110 kV and 1.5 mA, 80 kV and 2.8
 106 mA) was evaluated. For this purpose, 22 commercial dry-cured ham packages of approximately
 107 240 g (12 slices each) were used. Proteolysis was induced by spreading 0.125 mL of a
 108 proteolytic enzyme (Delvolase®, DSM Food Specialties, France) on each face (about 90 cm²) of
 109 the slices from the package. The slices were immediately piled and vacuum packaged again.
 110 This procedure facilitated the penetration of the enzyme and allowed a more homogeneous
 111 proteolysis generation in the package. Samples were kept vacuum packaged at 25°C to induce
 112 proteolysis and were scanned after 0, 2, 4, 6, 8, 24 and 48h. According to Rubio et al (2013),
 113 increase of the proteolytic induction time will produce a logarithmic increase of pastiness or
 114 defective texture level.

115 From each acquired spectroscopic image, the *Biceps femoris* (BF) muscle was manually
 116 selected and the mean attenuation spectrum (Eq. 1) for each energy band (Eq. 2) was calculated.
 117 Afterwards, salt and water contents of the BF muscle were then analytically determined.

118 **2.3.2 Characterization of dry-cured ham slices using multi energy X-ray spectra**

119 160 dry-cured hams were measured to evaluate the feasibility of the technology to characterize
 120 or classify samples according to their proteolysis index. 160 raw hams with a pH<5.5, which are
 121 more prone to developing defective textures, were obtained from a commercial slaughterhouse.
 122 All the hams (n = 160) were weighed (11.9 kg ± 1.1 kg) and salted according to the traditional
 123 system; hams were manually rubbed with the following mixture (g/kg of raw ham): 0.15 of
 124 KNO₃, 0.15 of NaNO₂, 1.0 of dextrose, 0.5 of ascorbic acid and 10 of NaCl. The hams were pile
 125 salted at 3 ± 2 °C and 85 ± 5% RH for 4 (n=40), 6 (n=40), 8 (n=40) or 11 days (n=40) to obtain
 126 samples with a broad range of salt content. After salting, hams were washed with cold water and
 127 post-salted at 3 ± 2 °C and 85 ± 5% RH for 45 days. The hams were then submitted to a drying
 128 process at 12 ± 2 °C and 70 ± 5% RH until reaching a weight loss of 29%. The hams were then
 129 vacuum packaged and kept at 30°C for 30 days to induce proteolysis (breakage of proteins) and
 130 to promote samples with a broad range of proteolysis index (defined as the ratio between non

131 protein nitrogen and total nitrogen). After this time, the drying process was continued at 12 ± 2
132 $^{\circ}\text{C}$ and $65 \pm 5\%$ RH until the hams reached a weight loss of 34%. The pieces were then vacuum
133 packaged again and kept at 30°C for 30 more days. After this period, the hams were dried again
134 until the end of process (considered when a weight loss of 36% was reached). At the end of the
135 process, the hams were boned and sampled.

136 2 cm thick slices from each ham were obtained and scanned at 110 kV and 1.5 mA (previously
137 established as the optimal). A ROI containing the BF muscle was selected, the mean attenuation
138 spectra was calculated as described in section 2.2 and pile up region discarded from the spectra.
139 Subsequently, instrumental texture, salt and water contents and proteolysis index of the BF
140 muscle were determined as described in section 2.4.

141 Samples were separated into different groups according to their proteolysis index, which is
142 known to be related to a defective texture (Ruiz-Ramírez, Arnau, Serra, & Gou, 2006; Ruiz-
143 Ramírez, Serra, Gou, & Arnau, 2006), for further statistical analysis. The following groups were
144 defined: Standard, $\text{PI} < 37\%$ and high defective, $\text{PI} > 37\%$.

145 **2.4 Physicochemical and sensory analysis**

146 Water content was analysed by drying at $103 \pm 2^{\circ}\text{C}$ until reaching a constant weight (AOAC,
147 1990). Chloride content was determined according to ISO 1841-2 using a potentiometric titrator
148 785 DMP Titrino (Metrohm AG, Herisau, Switzerland) and expressed as salt content. Non-
149 protein nitrogen content (NPN) was determined by precipitation of proteins with trichloroacetic
150 acid (Kerese, 1984) followed by determination of the total nitrogen (TN) in the extract with the
151 Kjeldahl method (AOAC, 2011). Proteolysis index (PI) was determined as a percentage of the
152 ratio between NPN and TN (Careri, et al., 1993; Schivazappa, et al., 2002). All the analyses
153 were performed in triplicate. Stress relaxation tests on BF muscles using parallelepipeds with
154 the same dimensions (2 cm x 2 cm x 1.5 cm) were performed. Initial force F_0 (kg) (representing
155 hardness) and force decay at 2 s (Y_2) and 90 s (Y_{90}) were calculated as previously described (R.
156 Morales, Guerrero, Serra, & Gou, 2007). A sensory analysis to evaluate pastiness, adhesiveness
157 and saliva viscosity was also carried out by an expert three-member panel trained following the
158 American Society for Testing and Materials standards (ASTM, 1981).

159 **2.5 Statistical analysis**

160 In order to evaluate the effect of the proteolytic induction (closely related to proteolysis
161 intensity) on the multi energy X-ray spectra, a two-way ANOVA was carried out including
162 proteolytic induction time as main effect and sample as block effect. Analyses were performed
163 on the following dependent variables: 1) attenuation of each channel of the spectra and 2)
164 attenuation of the energy bands calculated from the spectra (section 2.2), when using different
165 acquisition conditions. Differences between proteolytic induction times were tested by means of

166 Tukey test. In order to study the influence of salt and water contents on the evaluation of
167 proteolysis intensity, an ANCOVA analysis was performed including proteolytic induction time
168 as a fixed factor and salt and water contents as co-variables. Correlations between attenuation
169 and salt and water contents at different energy bands were also determined by Pearson product-
170 moment coefficient (r).

171 A partial least square regression (PLSR) analysis using all the channels of the spectra was
172 performed to develop the predictive models for estimating the proteolysis index in the
173 commercial ham samples. The 160 samples were split into two sets, 2/3 for the calibration (106
174 samples) and 1/3 for the validation (54 samples). To ensure a similar variation in composition in
175 the calibration and validation sets, a stratified sampling method was performed. Coefficient of
176 determination adjusted for degrees of freedom (R^2), standard error of calibration (RMSEC) and
177 standard error of validation (RMSEV) were calculated. A partial least square regression coupled
178 with a discriminant analysis (PLS-DA) was also used to determine the capacity of the model to
179 distribute samples into defective and non-defective groups according to their proteolysis index
180 level as established in section 2.3 and thus, to analyse the feasibility to separate highly defective
181 textural samples. All the analyses were performed using the statistical package XLSTAT
182 (Addinsoft, Paris, France).

183 **3. Results**

184 **3.1 Effect of induced proteolysis on spectra and energy bands**

185 Figure 3 shows the spectra of the intensity for the incident X-ray energies (dashed line) and the
186 mean attenuation spectra for *Biceps femoris* muscle obtained from the sliced dry-cured ham
187 after different proteolytic induction times (continuous lines) at different acquisition conditions.

188 At 140 and 110 kV, channels recording more than 1% of energy (channels from 1 to 48)
189 accounted for 75% of the total intensity of the incident X-rays (Figures 3 a and b, dashed line)
190 whereas at 80 kV, channels recording the total intensity of 85% were from 1 to 43 but the
191 intensity of the incident energy per channel varied from 1 to 2.7%, increasing in the first
192 channels and decreasing later on (Figure 3c, dashed line). As mentioned previously, the
193 acquisition conditions (voltage and intensity of X-ray tube) can produce different attenuation
194 responses (Fulladosa, et al., 2015; Håseth, et al., 2008) which may be more or less adequate to
195 characterize or detect induced proteolysis. In the case of multi energy sensors, as shown in
196 Figure 3, the spectra of the intensity for the incident X-ray energies influences the attenuation
197 produced. The level of white noise in the image is lower in low energy channels. This fact could
198 be attributed to the higher intensity of the incident X-rays at these energies in comparison to the
199 rest of channels (the main part of X-rays have low energies). For this reason, information from

200 the initial section of the spectra may provide more reliable information than that of the end part
201 of the spectra.

202 At 140 and 110 kV a similar attenuation pattern and a minimum peak of attenuation was
203 observed between channels 32 and 40 (energies 55 - 63 keV) (Figure 3a and 3b). In contrast, at
204 80 kV, a plateau of minimum attenuation was found between energy channels 20 and 40
205 (energies 41 - 63 keV) (Figure 3c). The attenuation response changed with the acquisition
206 conditions, probably due to the different intensity pattern of incident energy. From energy
207 channel 48 up to the last channel at 140 and 110 kV, and from 43 up to the last channel at 80
208 kV, information might be less reliable because of the high level of white noise in the images
209 obtained at these energies probably caused by the lower amount of incident energy intensity.
210 Information from the pile up region was not considered in the analysis (Figure 3, grey area). For
211 sliced dry-cured ham (at any proteolytic induction times) attenuation clearly decreased with
212 increasing X-ray energy as previously reported by other published works (Fulladosa, Santos-
213 Garcés, Picouet, & Gou, 2010; Håseth, et al., 2008). However, an increase of attenuation was
214 observed from energy channel 40 up to the end of the spectra. This fact may have been due to
215 the insufficient intensity of the incident X-rays, as previously described, which starts to decrease
216 steeply from this energy channel on. The attenuation of multi energy spectra clearly decreases
217 when increasing proteolysis and degradation of the tissue, in the entire spectra and at all
218 acquisition conditions (Figure 3). Statistical analysis showed a significant decrease of
219 attenuation with increasing proteolytic induction times ($p < 0.01$) for all the analysed energy
220 channels and emission conditions. Grouping channel information in energy bands facilitated the
221 comparison of the different regions of the spectra. At 140 kV, significant differences were
222 observed among most proteolysis induction times and for all EB (Table 1). At 110 kV, the same
223 previously described behaviour was observed (Table 2). However, acquisition at 110 kV was
224 more discriminant than 140 kV since F values were higher. In contrast, at 80 kV (Table 3), no
225 significant differences between 0 and 2 h, 4 and 6 h or 6 and 8 hours induction times were
226 observed for any of the energy bands considered. It is still unknown what kind of phenomenon
227 produce this decrease on attenuation. The attenuation of any material is basically caused by a
228 combination of photo-electric and Compton effects. The photo-electric effect predominates at
229 lower photon energies, is heavily energy dependant and is related to high atomic numbers.
230 Compton scattering occurs almost independently of the photon energy at energies exceeding 30
231 keV and is predominantly related to the density of the material. Therefore, the observed
232 decrease of attenuation could be attributed to the Compton scattering rather than the photo-
233 electric effect. Changes on the scattering of X-rays due to the changes in the cell structure were
234 suggested by Nielsen et al (2014) for frozen and defrosted fruit using dark-field radiography.
235 Variations of X-ray scattering have also been observed in bovine muscle structure due to protein

236 degradation using a small angle x-ray scattering synchrotron (Hoban, et al., 2016). Additionally,
237 breaking of molecules and structures caused by proteolysis (Fulladosa, et al., 2017) might
238 produce increased repulsion between molecules due to alteration in their molecular charges, and
239 thus of volume (not measurable) that could lead to a decrease of density in the sample and thus
240 of attenuation.

241 **3.2 Effect of sample composition on X-ray attenuation of induced proteolysis samples**

242 The effect of dry-cured ham composition (salt and water content) on the X-ray attenuation has
243 previously been reported previously for both dual energy (De Prados, et al., 2015; Fulladosa, et
244 al., 2015) and multi energy sensors (Fulladosa, Gou, & Muñoz, 2016). Therefore, when
245 analysing attenuation caused by proteolysis, sample compositions (salt and water contents)
246 influence the spectra.

247 No significant correlation was found between salt and water contents ($r=0.283$) in the samples
248 used to investigate the effect of proteolytic induction time. Statistical analysis of the effect of
249 different proteolytic induction times using water and salt contents as co-variables (ANCOVA)
250 showed a significant effect for both parameters in all the studied conditions. For all acquisition
251 conditions (80, 110 and 140 kV) and energy bands, a negative slope for water was observed
252 indicating that attenuation of spectra was negatively influenced by this parameter (an increase of
253 water produced a decrease of attenuation). In contrast, attenuation was positively influenced by
254 salt (an increase of salt produced an increase of attenuation). Because the slope value of salt
255 content was higher than that of water content, the influence of salt content on the spectra is
256 likely to be more relevant. For example, in the case of 110 kV, slope of salt content was 5.9, 3.2
257 and 2.7 times higher than that of water content for EB₁₋₂₀, EB₂₁₋₄₀ and EB₄₁₋₆₀, respectively.
258 However, it must be pointed out that the standard deviation of water content was 2.5 times
259 higher than that of salt content, hence the influence of both parameters on X-ray attenuation for
260 EB₄₁₋₆₀ was similar.

261 Besides, before proteolysis was induced in the samples, the highest correlation of salt with
262 attenuation ($r=0.529$) was found in EB₁₋₂₀ at 80 kV as previously reported by Fulladosa et al
263 (2016) and decreased for the other energy bands and acquisition conditions (Figure 4). For
264 water, the correlation with attenuation was lower (r between -0.299 and -0.414) with similar
265 values for the different acquisition conditions and energy bands. The lowest correlation for both
266 salt and water contents was observed in EB₂₀₋₄₁ at 110 kV. This result is in agreement with the
267 low slopes of salt and water from ANCOVA analysis. Therefore, the region of the spectra with
268 the least influence of salt and water is around channel 21 to 40 (X-ray energies between 43 and
269 64 keV) for emission conditions at 110 kV.

270 Other compositional variations and factors may significantly influence the acquired spectra.
271 Moreover, proteolysis intensities obtained by using the proteolytic enzyme were higher than
272 those found in commercial samples. For all these reasons, a validation using commercial-like
273 samples is needed in order to study the feasibility of this technology for characterizing texture
274 and/or detect textural defects in sliced dry-cured ham.

275 **3.3 Characterization and classification of samples by partial least square regression and** 276 **discriminant analysis**

277 Prediction and classification feasibility of commercial samples according to their proteolysis
278 index and defective texture was analysed using a PLSR and a PLS-DA analysis. As shown in
279 Table 4, the proteolysis index and sensory pastiness intensity of the non-induced samples used
280 in the study were significantly correlated ($r=0.568$) ($p<0.001$) (Table 4). Careri et al (1993) and
281 Arnau (1991) have already described this fact. This allows the use of the proteolysis index as a
282 chemical marker to characterize defective texture of dry-cured ham samples. Besides,
283 proteolysis index of the samples was also significantly correlated to instrumental texture
284 parameters ($r=0.682$ for Y_2 , $r=0.591$ for Y_{90} and $r=-0.636$ for F_0). Morales et al (2007) described
285 samples having low Y_{90} values as defective texture samples. In contrast, there was no
286 correlation between the proteolysis index and salt ($r=-0.031$) or water contents ($r=-0.008$),
287 despite proteolysis being sometimes related to a reduced salt content. The reason for this lack of
288 correlation was the experimental design used as it aimed at obtaining samples with textural
289 defects at different salt and water contents. This characteristic of the sample set is necessary to
290 estimate the sample proteolysis index and evaluate the feasibility of the technology avoiding
291 interference of composition (Fulladosa, et al., 2016).

292 Table 4 also shows the physicochemical characteristics of the samples used to develop PLSR
293 models. A wide variation of proteolysis index ranging from 26.71 to 45.03 was obtained, as well
294 as a wide variation of textural characteristics and salt and water contents. Developed PLSR
295 models using spectra acquired at 110kV to predict the proteolysis index of the samples were not
296 suitably robust. Figure 5 shows the RMSE of calibration and validation when using from 1 to 5
297 PLS factors. The minimum RMSE of calibration (3.16%) and validation (3.56%) were found
298 when using two PLS factors showing a R^2 of 0.436. The use of more data might improve the
299 robustness of predictive models.

300 The feasibility of discriminating samples in different groups using a PLS-DA model was also
301 evaluated. Table 5 shows the physicochemical characteristics of high defective and standard
302 samples sets. Significant differences of proteolysis index, F_0 , Y_2 and Y_{90} between defined sets
303 were obtained. Besides, the high defective set produced a decrease on the mean attenuation
304 spectra in comparison to the standard set (Figure 6). This fact was attributed to the proteolysis

305 index which was the only parameter significantly different between the two groups (Table 5).
306 Using a PLS-DA model, the overall correct classification score for the validation data set was
307 75.93% when using 15 PLS factors. However, a limited discrimination power for the high
308 defective samples was found, which obtained a classification correctness of only 44.44% (Table
309 6). This experiment should be evaluated using a higher number of samples in the defective
310 group. The use of more sophisticated algorithms, which for instance take into account the
311 relation between several regions of the spectra, could also achieve better prediction results.

312 **4. Conclusions**

313 Multi energy X-ray analysis is able to detect changes caused by induced proteolysis in sliced
314 dry-cured ham. The optimal acquisition conditions were 110 kV and 1.5 mA and changes were
315 preferably detected in the low energy section of the spectra. Because of the important
316 interference of salt and water contents on the X-ray attenuation, the ability of the technology to
317 estimate or discriminate commercial samples according to the proteolysis index level is limited.

318 **5. Acknowledgements**

319 This work was partially supported by INIA (contract n. RTA2013-00030-CO3-01), Ministerio
320 de Economía y Competitividad (PEJ-2014-A34573) and CERCA programme from Generalitat
321 de Catalunya.

322 **6. References**

- 323 AOAC (1990). Official method 950.46, Moisture in meat, B. Air drying.
- 324 AOAC (2011). Official method 2011.04, Protein in Raw and Processed Meats.
- 325 Arnau, J. (1991). *Aportacions a la qualitat tecnològica del jamón curado elaborado por*
326 *procesos acelerados*. . Universitat Autònoma de Barcelona.
- 327 ASTM. (1981). American Society for Testing and Materials. Guidelines for the
328 selection and training of sensory panel members. ASTM STP 758. In. ASTM,
329 Philadelphia, p. 33.
- 330 Careri, M., Mangia, A., Barbieri, A., Bolzoni, L., Virgili, R., & Parolari, G. (1993).
331 Sensory property relationships to chemical data of italian-type dry-cured ham.
332 *Journal of Food Science*, 58(5), 968-972.
- 333 Damez, J.-L., & Clerjon, S. (2013). Quantifying and predicting meat and meat products
334 quality attributes using electromagnetic waves: An overview. *Meat Science*, 95(4),
335 879-896.
- 336 De Prados, M., Fulladosa, E., Gou, P., Muñoz, I., Garcia-Perez, J. V., & Bedito, J.
337 (2015). Non-destructive determination of fat content in green hams using
338 ultrasound and X-rays. *Meat Science*, 104, 37-43.
- 339 Font-i-Furnols, M., Fulladosa, E., Prevolnik, M., & Candek Potokar, M. (2015). Future
340 trends in non-invasive technologies suitable for quality determinations. In *A*
341 *Handbook of Reference Methods for Meat Quality Assessment* (pp. 90-103).
342 Brussels, Belgium: COST Action FA1102, FAIM.
- 343 Fulladosa, E., de Prados, M., García-Perez, J. V., Bedito, J., Muñoz, I., Arnau, J., &
344 Gou, P. (2015). X-ray absorptiometry and ultrasound technologies for non-

- 345 destructive compositional analysis of dry-cured ham. *Journal of Food Engineering*,
346 155, 62-68.
- 347 Fulladosa, E., Gou, P., & Muñoz, I. (2016). Effect of dry-cured ham composition on X-
348 ray multi energy spectra. *Food Control*, 70, 41-47.
- 349 Fulladosa, E., Rubio-Celorio, M., Skytte, J. L., Muñoz, I., & Picouet, P. (2017). Laser-
350 light backscattering response to water content and proteolysis in dry-cured ham.
351 *Food Control*, 77, 235-242.
- 352 Fulladosa, E., Sala, X., Gou, P., Garriga, M., & Arnau, J. (2012). K-lactate and high
353 pressure effects on the safety and quality of restructured hams. *Meat Science*, 91(1),
354 56-61.
- 355 Fulladosa, E., Santos-Garcés, E., Picouet, P., & Gou, P. (2010). Prediction of salt and
356 water content in dry-cured hams by computed tomography. *Journal of Food*
357 *Engineering*, 96(1), 80-85.
- 358 García-Rey, R. M., García-Olmo, J., Pedro, E., Quiles-Zafra, R., & Castro, M. D. L.
359 (2005). Prediction of texture and colour of dry-cured ham by visible and near
360 infrared spectroscopy using a fiber optic probe. *Meat Science*, 70, 357-363.
- 361 Guerrero, L., Gobantes, I., Oliver, M. A., Arnau, J., Guàrdia, M. D., Elvira, J., Riu, P.,
362 Grèbol, N., & Monfort, J. M. (2004). Green hams electrical impedance
363 spectroscopy (EIS) measures and pastiness prediction of dry cured hams. *Meat*
364 *Science*, 66, 289-294.
- 365 Håseth, T., Høy, M., Kongsro, J., Kohler, A., Sørheim, O., & Egelanddal, B. (2008).
366 Determination of sodium chloride in pork meat by computed tomography at
367 different voltages. *Journal of Food Science*, 73(7), 333-339.
- 368 Hoban, J. M., Hopkins, D. L., Kirby, N., Collins, D., Dunshea, F. R., Kerr, M. G.,
369 Bailes, K., Cottrell, J. J., Holman, B. W. B., Brown, W., & Ponnampalam, E. N.
370 (2016). Application of small angle X-ray scattering synchrotron technology for
371 measuring ovine meat quality. *Meat Science*, 117, 122-129.
- 372 ISO 1841-2 (1996). Meat and Meat Products. Determination of Chloride Content -Part 2:
373 Potentiometric Method (Reference method). Geneva: International Organization for
374 Standardization
- 375 ISO 937:1978. Meat and meat products. Determination of nitrogen content (Reference method).
376 International Organization for Standardization, Geneva.
- 377 Kerese, I. 1984. Methods of protein analysis. Chichester: Ellis Howood Ltd.
- 378 McCollough, C., Leng, S., Yu, L., & Fletcher, J. G. (2015). Dual- and Multi-Energy
379 Computed Tomography: Principles, Technical Approaches, and Clinical
380 Applications. *Radiology*, 276(3), 637-653.
- 381 Morales, Arnau, J., Serra, X., Guerrero, L., & Gou, P. (2008). Texture changes in dry-
382 cured ham pieces by mild thermal treatments at the end of the drying process. *Meat*
383 *Science*, 80, 231-238.
- 384 Morales, Guerrero, L., Claret, A., Guàrdia, M. D., & Gou, P. (2008). Beliefs and
385 attitudes of butchers and consumers towards dry-cured ham. *Meat Science*, 80(4),
386 1005-1012.
- 387 Morales, R., Guerrero, L., Serra, X., & Gou, P. (2007). Instrumental evaluation of
388 defective texture in dry-cured hams. *Meat Science*, 76, 536-542.
- 389 Nielsen, M. S., Christensen, L. B., & Feidenhans'l, R. (2014). Frozen and defrosted fruit
390 revealed with X-ray dark-field radiography. *Food Control*, 39, 222-226.
- 391 Ortiz, M. C., Sarabia, L., García-Rey, R., & Castro, M. D. L. (2006). Sensitivity and
392 specificity of PLS-class modelling for five sensory characteristics of dry-cured ham

- 393 using visible and near infrared spectroscopy. *Analytica Chimica Acta*, 558, 125-
394 131.
- 395 Rubio-Celorio, M., Fulladosa, E., Claret, A., Guàrdia, M. D. a., & Garcia-Gil, N.
396 (2013). Detection of pastiness in dry-cured ham using dielectric time domain
397 reflectometry. *59th International Congress of Meat Science and Technology -*
398 *ICoMST 2013, Izmir, Turkey, 2013*.
- 399 Ruiz-Ramírez, J., Arnau, J., Serra, X., & Gou, P. (2006). Effect of pH₂₄, NaCl content
400 and proteolysis index on the relationship between water content and texture
401 parameters in biceps femoris and semimembranosus muscles in dry-cured ham.
402 *Meat Science*, 72, 185-194.
- 403 Ruiz-Ramírez, J., Serra, X., Gou, P., & Arnau, J. (2006). Efecto del índice de proteolisis
404 sobre la textura del jamón crudo curado. *Archivos Latinoamericanos de Produccion*
405 *Animal*, 14(2), 62-64.
- 406 Schivazappa, C., Degni, M., Costa, L. N., Russo, V., Buttazoni, L., & Virgili, R. (2002).
407 Analysis of raw meat to predict proteolysis in Parma ham. *Meat Science*, 60, 77-83.
- 408 Skrlep, M., Candek-Potokar, M., Mandelc, S., Javornik, B., Gou, P., Chambon, C., &
409 Sante-Lhoutellier, V. (2011). Proteomic profile of dry-cured ham relative to
410 PRKAG3 or CAST genotype, level of salt and pastiness. *Meat Science*, 88(4), 657-
411 667.
- 412 Tapiador Farelo, J., & García Garrido, J. A. (2003). Avances en la ciencia, tecnología y
413 comercialización del jamón (Cojamón 2003, Cáceres) In (pp. 70-77).

414
415

1 TABLES

2

3 **Table 1.** Mean and standard deviation of the attenuation for different energy bands of the spectra when emitting at 140 kV and 1 mA after different proteolysis
4 induction times (n=22).

Time of enzyme exposure	EB ₁₋₂₀		EB ₂₁₋₄₀		EB ₄₁₋₆₀		EB ₆₁₋₈₀		EB ₈₁₋₁₀₀	
	Mean	SD	Mean	SD	Mean	SD	Mean	SD	Mean	SD
0 h	0.272 ^a	0.044	0.160 ^a	0.037	0.192 ^a	0.030	0.237 ^a	0.018	0.301 ^a	0.036
2 h	0.266 ^b	0.043	0.156 ^b	0.036	0.190 ^a	0.030	0.235 ^a	0.018	0.300 ^a	0.037
4 h	0.259 ^c	0.042	0.152 ^{bc}	0.035	0.185 ^b	0.029	0.229 ^b	0.019	0.292 ^b	0.037
6 h	0.254 ^{cd}	0.042	0.149 ^{cd}	0.035	0.182 ^{bc}	0.030	0.225 ^{bc}	0.020	0.288 ^b	0.037
8 h	0.249 ^d	0.041	0.146 ^d	0.034	0.177 ^c	0.029	0.219 ^c	0.019	0.279 ^c	0.035
24 h	0.237 ^e	0.042	0.139 ^e	0.033	0.170 ^d	0.029	0.211 ^d	0.021	0.270 ^d	0.037
48 h	0.227 ^f	0.041	0.133 ^f	0.032	0.163 ^e	0.029	0.203 ^c	0.022	0.260 ^c	0.037

5 ^{a-f}Different letters indicate significant differences (p<0.05) between proteolysis induction times within each calculated energy band. SD: Standard deviation;
6 EB: Energy band.

7

8

9 **Table 2.** Mean and standard deviation of the attenuation for different energy bands of the spectra when emitting at 110 kV and 1.5 mA after different
10 proteolysis induction times (n=22).

Time of enzyme exposure	EB ₁₋₂₀		EB ₂₁₋₄₀		EB ₄₁₋₆₀		EB ₆₁₋₈₀	
	Mean	SD	Mean	SD	Mean	SD	Mean	SD
0 h	0.297 ^a	0.062	0.179 ^a	0.028	0.221 ^a	0.032	0.326 ^a	0.054
2 h	0.289 ^b	0.060	0.175 ^b	0.027	0.218 ^a	0.032	0.324 ^a	0.055
4 h	0.282 ^c	0.059	0.170 ^c	0.027	0.212 ^b	0.032	0.315 ^b	0.054
6 h	0.278 ^c	0.060	0.169 ^c	0.028	0.210 ^b	0.033	0.313 ^b	0.054
8 h	0.270 ^d	0.058	0.163 ^d	0.027	0.202 ^c	0.031	0.299 ^c	0.051
24 h	0.258 ^e	0.057	0.156 ^e	0.027	0.195 ^d	0.032	0.290 ^d	0.053
48 h	0.248 ^f	0.056	0.150 ^f	0.026	0.188 ^e	0.031	0.280 ^e	0.051

11 ^{a-f}Different letters indicate significant differences (p<0.05) between proteolysis induction times within each calculated energy band. SD: Standard deviation;
12 EB: Energy band.

13
14

15 **Table 3.** Mean and standard deviation of the attenuation for different energy bands of the spectra when emitting at 80 kV and 2.8 mA after different
 16 proteolysis induction times (n=22).

Time of enzyme exposure	EB ₁₋₂₀		EB ₂₁₋₄₀		EB ₄₁₋₆₀	
	Mean	SD	Mean	SD	Mean	SD
0 h	0.332 ^a	0.087	0.224 ^a	0.017	0.419 ^a	0.129
2 h	0.326 ^a	0.085	0.220 ^a	0.017	0.416 ^a	0.126
4 h	0.317 ^b	0.083	0.214 ^b	0.017	0.405 ^b	0.124
6 h	0.315 ^{bc}	0.081	0.211 ^{bc}	0.013	0.396 ^{bc}	0.120
8 h	0.303 ^c	0.081	0.204 ^c	0.018	0.383 ^{cd}	0.118
24 h	0.290 ^d	0.080	0.196 ^d	0.020	0.374 ^d	0.117
48 h	0.278 ^e	0.078	0.189 ^e	0.021	0.359 ^e	0.113

17 ^{a-e}Different letters indicate significant differences (p<0.05) between proteolysis induction times within each calculated energy band. SD: Standard deviation;
 18 EB: Energy band.

19
 20

21

22

23

Table 4. Physicochemical characterization of non-induced samples used to develop and validate PLSR predictive models to determine proteolysis index as a biochemical indicator of dry-cured ham texture.

	Mean	Standard deviation	min	max	Pearson correlation coefficients							
					Proteolysis index (%)	Salt content (%)	Water content (%)	F ₀	Y ₂	Y ₉₀	Pastiness perception	
Proteolysis index (%)	34.79	3.71	26.71	45.03	1							
Salt content (%)	4.76	0.86	2.97	6.93	-0.181	1						
Water content (%)	58.89	0.98	55.98	61.76	-0.060	-0.397	1					
F ₀	1.24	0.69	0.221	3.55	-0.634	0.278	-0.260	1				
Y ₂	0.39	0.037	0.309	0.483	0.594	-0.168	0.168	-0.896	1			
Y ₉₀	0.67	0.030	0.589	0.745	0.534	-0.262	0.213	-0.875	0.963	1		
Pastiness perception	1.25	1.39	0	6	0.568	-0.031	-0.008	-0.636	0.682	0.590	1	

24

25

26

27

28

29

Table 5. Physicochemical characterization of high defective and standard texture groups used to develop and validate models to discriminate non-induced samples according to texture.

Sample set	n	Proteolysis index (%)				Salt content (%)		Water content (%)		F ₀		Y ₂		Y ₉₀	
		Mean	SD	Min	Max	Mean	SD	Mean	SD	Mean	SD	Mean	SD	Mean	SD
High defective	29	40,04 ^a	2,02	37,26	45,03	4,66	0,83	58,84	1,13	0,74 ^a	0,37	0,42 ^a	0,03	0,69 ^a	0,03
Standard	134	33,16 ^b	2,51	26,71	36,94	4,87	0,86	58,89	0,93	1,43 ^b	0,67	0,38 ^b	0,04	0,67 ^b	0,03

30

31

32

33

34

35

36

37

38

39

40

Table 6. Classification performance of standard and high defective dry-cured ham samples using PLS-DA.

	Standard	High defective	total	% Correctness
Standard	37	8	45	82.22
High defective	5	4	9	44.44
total	42	12	54	75.93

41

1 FIGURES

2

3

4

5

6

7

8

9

10

11

12

13

14

15

16

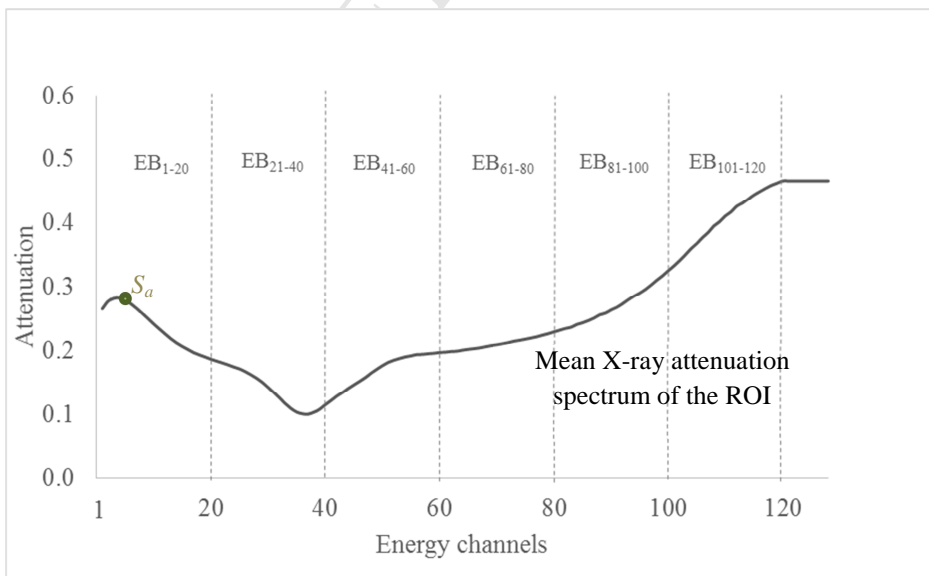
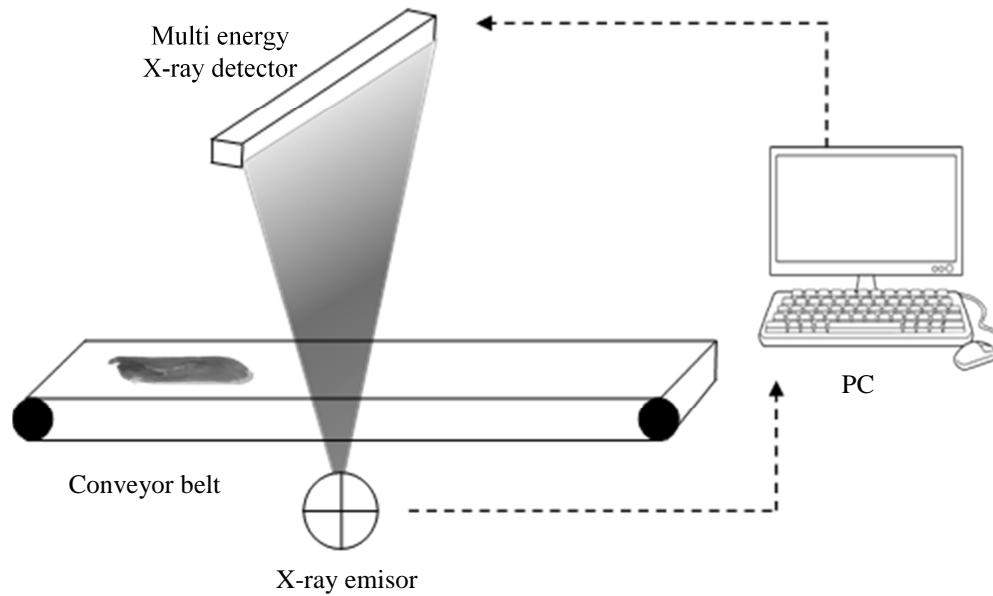
17

18

19 **Figure 1.** X-ray prototype system with a multi energy detector.

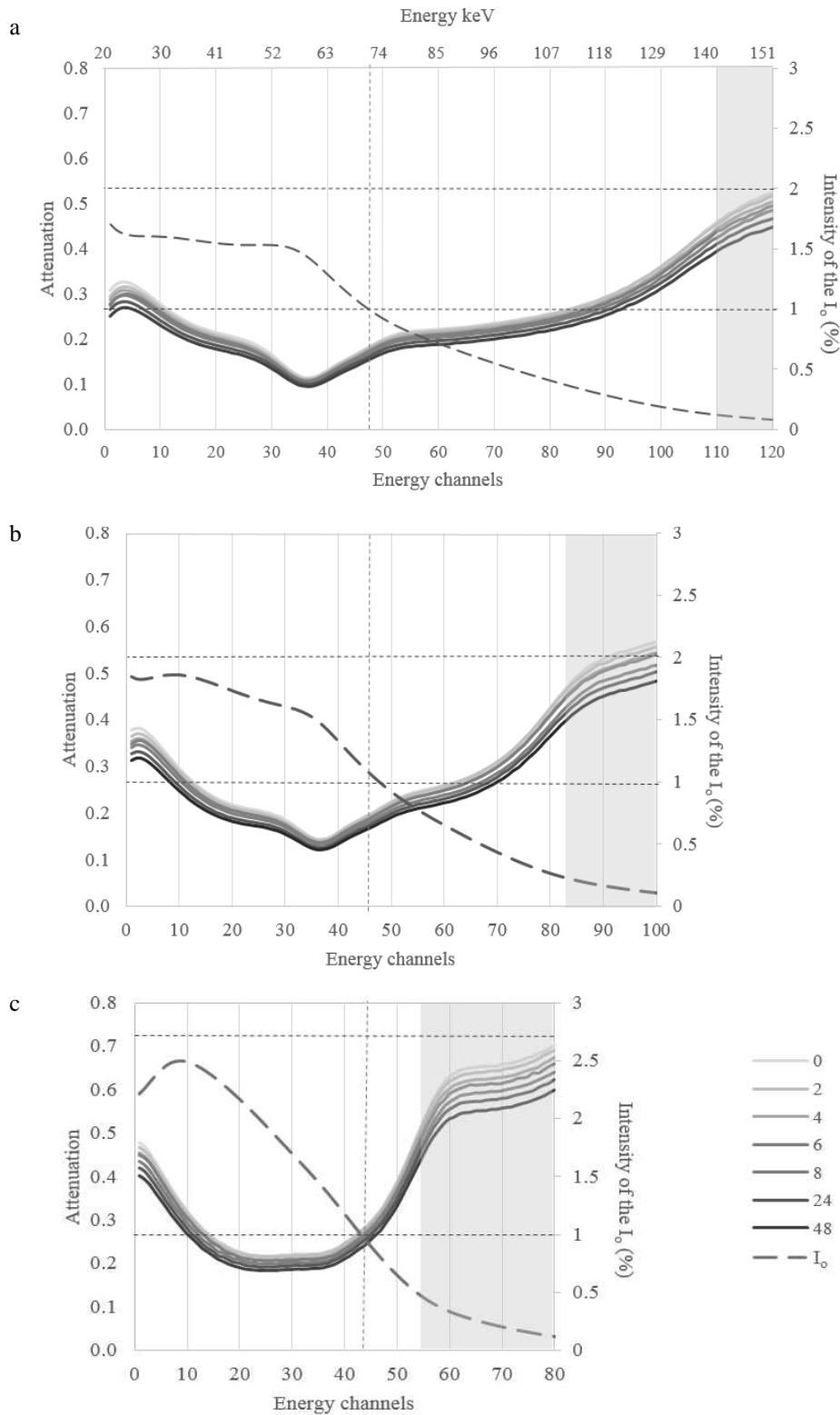
20

21



22

23 **Figure 2.** Representation of a mean X-ray attenuation spectrum of a ROI obtained by a multi
24 energy X-ray device. EB: energy band; S_a : Attenuation value for a given energy channel a .

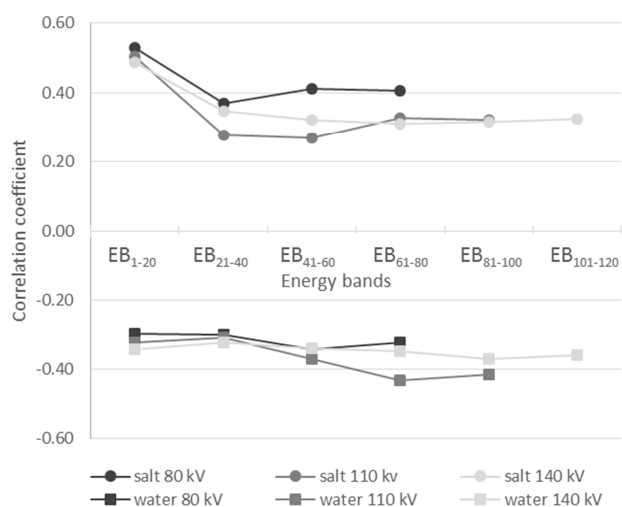


25

26 **Figure 3.** Mean X-ray attenuation spectra obtained from *Biceps femoris* muscle of sliced dry-
 27 cured ham after different proteolysis induction times (0, 2, 4, 6, 8, 24 and 48 h) when emitting at
 28 140 kV and 1 mA (a), 110 kV and 1.5 mA (b) and 80 kV and 2.8 mA (c). Intensity of the
 29 incident X-rays of different energy (I_0) at the corresponding emission conditions is also showed.
 30 Grey area corresponds to pile up region.

31

32



33

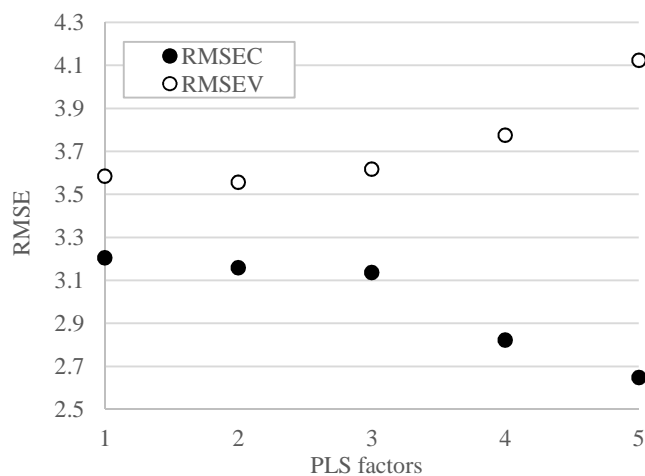
34 **Figure 4.** Correlation coefficients between attenuation and salt and water contents for the
 35 different energy bands when using spectra acquired from samples before proteolysis induction
 36 at different acquisition conditions (140, 110 and 80 kV).

37

38

39

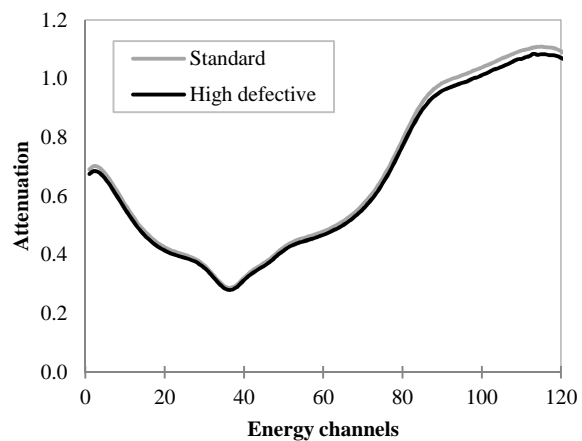
40



41

42 **Figure 5.** Variation of Root mean square errors (RMSE) for calibration and validation data sets
 43 when using different number of PLS factors.

44



45
46 **Figure 6.** Mean X-ray attenuation spectrum for standard (IP<37%) and high defective (IP>37%)
47 data sets acquired at 110 kV and 1.5 mA.

48

Highlights

Increase of proteolysis decreases X-ray attenuation

The decrease in attenuation depends on the energy band

Salt interferes more than water in the prediction of proteolysis index

Classification performance of proteolysis index of commercial was limited

ACCEPTED MANUSCRIPT